Journal of Inorganic Biochemistry 220 (2021) 111464

Contents lists available at ScienceDirect

Journal of Inorganic Biochemistry

journal homepage: www.elsevier.com/locate/jinorgbio

Two Cu(II) coordination polymers: Heterogeneous catalytic Knoevenagel condensation reaction and treatment activity on atherosclerosis via regulating the expression of the COX-2 in vascular endothelial cells

Yong-Chang Zhao [a], Yan Zhang [b], De-Ying Jiang [c,*], Liang Wang [d], Ping Sun [d]

[a] Imaging Intervention Room, 3201 Hospital of Xi'an Jiaotong University, Hanzhong, Shaanxi, China
[b] Internal Courage, Hiser Hospital of Qingdao City, Qingdao, Shandong, China
[c] Vascular Surgery, Dalian Municipal Central Hospital, Dalian, Liaoning, China
[d] Department of Chemistry, Capital Medical University, Beijing, China

ARTICLE INFO

Keywords:
Coordination polymers
X-ray diffraction
Heterogeneous catalyst
Atherosclerosis

ABSTRACT

By altering auxiliary nitrogen-donor ligands, two novel coordination polymers (CPs) containing Cu(II) formulated as $[Cu_{2.5}(L)(trz)_2(H_2O)_2]\cdot 2H_2O$ (**1**) (Htrz = 1,2,4-triazole and H_3L = 5-(4-carboxybenzyloxy)isophthalic acid) and [Cu(HL)(Hbiz)] (**2**, Hbiz = benzimidazole) have been produced under the hydrothermal conditions. The complex **2** with both acidic and basic sites was investigated as heterogeneous catalyst, which reveals highly efficient catalytic property of the Knoevenagel condensation reaction. Dynamic changes of coagulation parameters during atherosclerosis was also explored via detecting activated partial thromboplastin time (APTT) and prothrombin time (PT), and the results showed that compared with CP **2**, CP **1** has a stronger improvement on the coagulation parameters during atherosclerosis. Then, the high-sensitivity C-reactive protein and matrix metalloproteinase-1 released by the atherosclerotic segment was detected with enzyme linked immunosorbent assay (ELISA) detection, which also revealed that CP **1** could obviously decrease the inflammatory mediator released by the atherosclerotic segment, but not CP **2**. And, the cyclooxygenase-2 (COX-2) relative expression level in vascular endothelial cells was detected via the real time RT-PCR. The results of the real time reverse transcription-polymerase chain reaction (RT-PCR) indicated that CP **1** has stronger activity on inhibiting the Notch signaling pathway than CP **2**. Finally, we got this information, CP **1** has excellent application values on the coagulation parameters during atherosclerosis via regulating the expression of the COX-2 in vascular endothelial cells.

1. Introduction

Atherosclerosis is a cardiovascular disease that seriously threatens human's health. At present, many cardiovascular diseases are closely related to atherosclerosis. For example, acute coronary syndrome (ACS) is a concurrent plaque rupture or erode based on coronary atherosclerosis, leading to acute or subacute reduced myocardial oxygen supply [1,2]. Therefore, the prevention and treatment of atherosclerosis has become the basis for the prevention of coronary heart disease. Up to now, the cause of atherosclerosis is not very clear. Atherosclerosis is a chronic inflammatory response, and inflammation is playing an increasingly important role in atherosclerosis [3]. Recent studies have shown that cyclooxygenase-2 (COX-2) is closely related to the inflammatory response to atherosclerosis.

Coordination polymers (CPs) composed of metal ions and organic ligands have gained great attentions in recent years for their rich potential applications in many important fields especially in catalysis and biomedicine [4–8]. The inherent properties of CPs such as highly dense active sites, endless selection of building blocks and robust frameworks make them excellent catalysts. The Knoevenagel condensation is a classic reaction, which provides an effective way to form C—C double bonds by the reaction of carbonyl compounds, such as aldehydes or ketones, with compounds containing active methylene groups. It has been widely used in the synthesis of many compounds and is a reaction with an important application value in organic synthesis [9–11]. In recent years, many catalysts for such reactions have emerged, among which CPs-based catalysts have shown remarkable catalytic performance. According to the literature, basic catalysis and bifunctional

* Corresponding author.
E-mail address: Lnjdy1977@163.com (D.-Y. Jiang).

https://doi.org/10.1016/j.jinorgbio.2021.111464
Received 26 December 2020; Received in revised form 7 April 2021; Accepted 8 April 2021
Available online 21 April 2021

acid–base catalysis are two generally accepted mechanisms for CPs-based catalysts in the Knoevenagel condensation, among which the construction of bifunctional acid–base catalysts is more challenge because this requires the combination of acidic and basic sites in one catalyst [12]. The acid-base mixed-ligand approach might be a feasible approach for building the bifunctional acid–base catalyst considering the potential undeprotonated carboxylate groups along with the uncoordinated N-donor sites. On the other hand, copper is an essential trace metal element in the human body Modern medical research shows that copper complexes can produce antibacterial, antiviral, anti-inflammatory, antitumor, enzyme inhibitory or chemical nuclease activities, which are increasingly attracting the attention of researchers [13–17]. Another drive for targeting copper(II) was due to its less toxic nature, which can be further decreased on complexation with ligands and thus proved promising in the development of copper complexes as bioactive agents [18]. Considering the above aspects, in this study, two new coordination polymers containing Cu(II) ions as nodes formulated as $[Cu_{2.5}(L)(trz)_2(H_2O)_2]\cdot 2H_2O$ (**1**) (Htrz = 1,2,4-triazole and H_3L = 5-(4-carboxybenzyloxy)isophthalic acid) and [Cu(HL)(Hbiz)] (**2**, Hbiz = benzimidazole) have been produced under the hydrothermal conditions, and their structures could be modulated using different auxiliary nitrogen-donor ligands. The complex **2** with both acidic and basic sites was investigated as heterogeneous catalyst, which reveals the highly efficient catalytic property of the Knoevenagel condensation reaction. The treatment effect of CPs against the atherosclerosis was evaluated and the particular mechanism was investigated as well. The results of activated partial thromboplastin time (APTT) and prothrombin time (PT) revealed that in comparison with CP **2**, CP **1** has a stronger improvement on the coagulation parameters during atherosclerosis. Besides, the enzyme linked immunosorbent assay (ELISA) assay also revealed that CP **1** could obviously decrease the inflammatory mediator released by the atherosclerotic segment, but not CP **2**. Following that, the COX-2 in vascular endothelial cells was also inhibited by CP **1** instead of CP **2**. Eventually, the western blot indicated that CP **1** has stronger activity on inhibiting the Notch signaling pathway.

2. Experimental

2.1. Chemicals and measurements

All chemicals were commercially available and they were used without further purification. The H_3L ligand was acquire from the Jinan Henghua Chemical Reagent company (Jinan, China). Nitrogen, hydrogen and carbon elements were analyzed via utilizing a analyzer of PerkinElmer 240C. The infrared spectra from 4000 to 400 cm^{-1} were recorded on the spectrometer of Bruker ALPHA utilizing pure solid samples. Via GC contains FID detector (GC-2014C, Shimadzu, Japan) and capillary (30 m long × 0.25 mm inner diameter, WondaCap 17), we calculated the conversion for catalytic reaction.

2.2. Preparation and characterization for $[Cu_{2.5}(L)(trz)_2(H_2O)_2]\cdot 2H_2O$ (1) and [Cu(HL)(Hbiz)] (2)

For the synthesis of CP **1**, a mixture of $Cu(NO_3)_2\cdot 3H_2O$ (0.50 mmol, 0.12 g), H_3L (0.35 mmol, 0.11 g), Htrz (0.35 mmol, 0.024 g), NaOH (0.50 mmol and 0.20 g) and H_2O (14 mL) was sealed into the stainless steel container of 25 mL lined with Teflon, the mixture was heated for 72 h at 150 °C and then cooled at 5 °C·h^{-1} rate to the ambient temperature. Blue crystals with block-shape of the CP **1** were harvested and cleaned by the distilled water and then dried in the air to obtain product; the yield is 36% (on the basis of Cu^{II} salts). Elemental analyses calcd (%) for $C_{40}H_{42}N_{12}O_{22}Cu_5$ (1360): C, 35.31; H, 3.11; N, 12.35. Found C, 35.41; H, 3.02; N, 12.13. IR (KBr pellet, cm^{-1}): 3320 (s), 3080 (w), 1766 (s), 1649 (s), 1551 (m), 1420 (w), 1250 (s), 1200 (s), 1055 (m), 1026 (m), 910 (m), 750 (s), 650 (w).

For the synthesis of CP **2**, a mixture of $Cu(NO_3)_2\cdot 3H_2O$ (0.50 mmol, 0.12 g), H_3L (0.35 mmol, 0.11 g), biz (41 mg, 0.35 mmol), NaOH (14 mg, 0.35 mmol) and H_2O (14 mL) was sealed into the stainless steel container of 25 mL lined with Teflon, the mixture was heated for 72 h at 150 °C and then cooled at 5 °C·h^{-1} rate to the ambient temperature. Blue crystals with block-shape of CP **2** were harvested and cleaned by the distilled water and then dried in the air to obtain product; the yield is 41.2% (on the basis of Cu^{II} salts). Elemental analyses calcd (%) for $C_{23}H_{16}N_2O_7Cu$ (495): C, 55.70; H, 3.25; N, 5.65. Found C, 55.59; H, 3.22; N, 5.57. IR (KBr pellet, cm^{-1}): 2965 (w), 1734 (s), 1690 (s), 1598 (s), 1460 (m), 1285 (s), 1206 (s), 1121 (m), 1057 (m), 889 (w), 765 (m), 664 (w), 531 (w).

The software of crysalispro was applied to analyze the strength data and then convert strength data into the HKL files. Via using the diffractometer of Oxford XcaliburE we acquired the data of X-ray. The program of SHELXS in accordance with the direct method was applied to construct the initial skeleton pattern for the CP 1, and the program of SHELXL-2014 in accordance with least square means was modified. Mixing the anisotropic parameters with the non-hydrogen atoms of CP **1**. Then all of the hydrogen atom via applying the command of AFIX to fix on the C atom geometrically they are connected to. The refinement along with the crystallographic parameters for the two CPs are described in detail in Table 1.

Table 1
The parameters of crystallography as well as the refinement for the two CPs.

Identification code	1	2
Empirical formula	$C_{40}H_{42}Cu_5N_{12}O_{22}$	$C_{23}H_{16}CuN_2O_7$
Formula weight	1360.55	495.92
Temperature/K	293(2)	293(2)
Crystal system	monoclinic	monoclinic
Space group	$P2_1/c$	$P2_1/c$
a/Å	11.369(2)	14.569(2)
b/Å	15.621(5)	7.652(3)
c/Å	13.2958(10)	17.996(2)
α/°	90	90
β/°	93.973(4)	107.9650(10)
γ/°	90	90
Volume/$Å^3$	2355.7(9)	1908.4(8)
Z	2	4
ρ_{calc}g/cm^3	1.918	1.726
μ/mm^{-1}	2.321	1.199
Data/restraints/ parameters	5701/6/390	3538/0/302
Goodness-of-fit on F^2	1.021	1.008
Final R indexes [$I \geq 2\sigma$ (I)]	R_1 = 0.0252, ωR_2 = 0.0586	R_1 = 0.0377, ωR_2 = 0.0714
Final R indexes [all data]	R_1 = 0.0359, ωR_2 = 0.0622	R_1 = 0.0659, ωR_2 = 0.0795
Largest diff. peak/hole/e $Å^{-3}$	0.34/−0.40	0.30/−0.33
CCDC	2,002,951	2,002,952

2.3. Knoevenagel condensation

All the experiments were carried out in a round bottom flask (10 mL) placed in a silicone bath under nitrogen atmosphere. Typically, 10 mmol of malononitrile as methylene compound, 2 mL of solvent (if used) and catalyst were added at room temperature. Thereafter, the mixture was heated up to the reaction temperature. Once the desired temperature was achieved, 10 mmol of benzaldehyde was added. The influence of reaction solvent and temperature was explored as listed in the Table 2. A stirring speed of 1000 rpm was fixed in order to avoid mass transfer limitations. Reactant and product concentrations were quantified by GC, ^1H NMR and ^{13}C NMR (Figs. S1–S9). Dodecane was used as an internal standard.

2.4. Coagulation parameters

In the process of the atherosclerosis, there was commonly combined

Table 2
The Knoevenagel reactions catalyzed under different conditions.

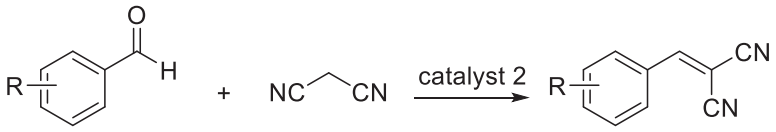

Entry	Catalyst	Dose (mg)	Temperature (°C)	Solvent	Conversion (%)
1	Blank	0	60	–	18
2	H_3L	3	60	–	52
3	benzimidazole	2	60	–	46
4	2	3	60	–	39
5	2	5	60	–	82
6	2	8	60	–	94
7	2	10	60	–	>99
8	2	10	RT	–	33
9	2	10	40	–	83
10	2	10	50	–	96
11	2	10	60	C_2H_5OH	78
12	2	10	60	CH_3COCH_3	20
13	2	10	60	CH_2Cl_2	18
14	2	10	60	$C_6H_5CH_3$	30
15	Htrz	10	50	–	43
16	1	10	50	–	20

with a dysregulated coagulation in the atherosclerotic segment, reflected as the reduced activated partial thromboplastin time (APTT) and prothrombin time (PT), which were both the standard coagulation parameters. Thus, in this experiment, CPs **1** and **2** were used for indicated treatment, and the PT, APTT values were measured. In brief, twenty healthy New Zealand male white rabbits were utilized as the experimental animals, and fed with high-fat diet, followed by treated with hypertension on one side of the renal artery stenosis to induce the animal model of atherosclerosis. Then these two CPs were given to perform the indicated treatment with a concentration of 5 mg/kg. All of preformation in this study were authorized via Zhejiang University Animal Ethics Committee (Hangzhou, China). Finally, animals' blood was collected and the PT and APTT values were measured at least three times.

2.5. ELISA assay

The ELISA test was also carried out in this study for the content of the high-sensitivity C-reactive protein and matrix metalloproteinase-1 released by the atherosclerotic segment into plasma. This detection was carried out totally according to instructions' guidance with slight modifications. In short, New Zealand white rabbits were fed by using high-fat diet and treated with hypertension on one side of the renal artery stenosis to induce the animal model of atherosclerosis. Then these two CPs were given for the indicated treatment with a concentration of 5 mg/kg. Next, the plasma of all the animals were collected and the level

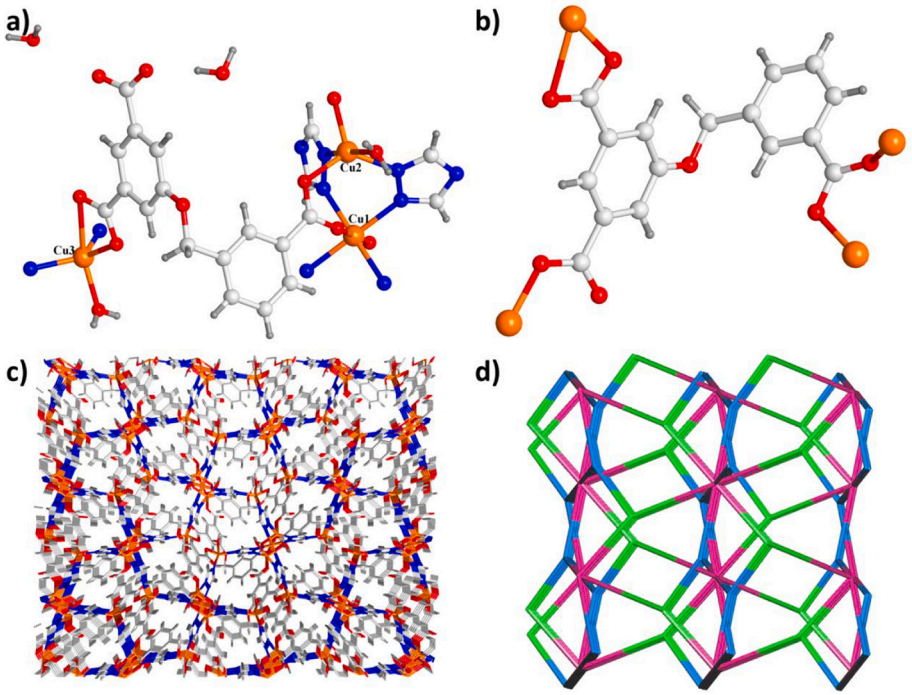

Fig. 1. (a) The coordination surroundings for Cu(II) ions in CP **1**. (b) The coordination diagrams of the ligand in the CP **1**. (c) The single network for CP **1**. (d) The (3,8)-linked net of CP **1**.

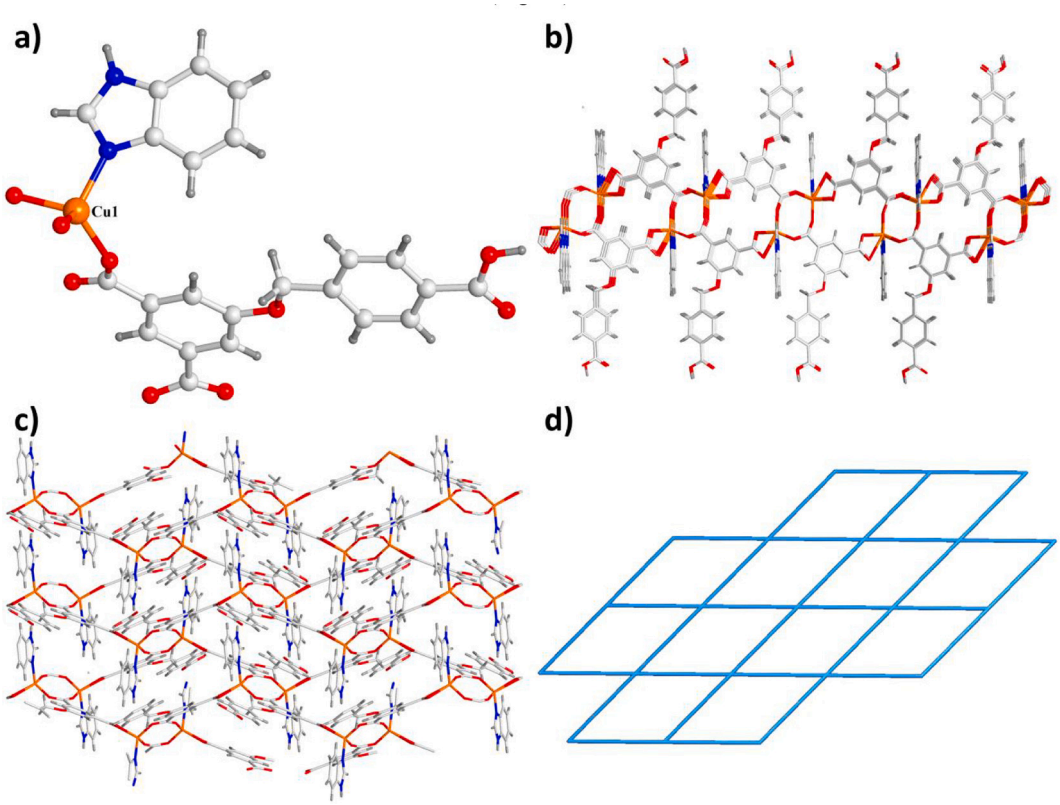

Fig. 2. (a) The asymmetric unit of CP **2**. The two-dimensional skeleton of CP **2** viewed along axis b (b) and a (c). (d) The (4)-linked two-dimensional net of CP **2**.

of the high-sensitivity C-reactive protein and matrix metalloproteinase-1 was detected through the indicated ELISA kit. This experiment was performed three times or more, and obtained results were expressed as mean ± standard deviation.

2.6. Real time reverse transcription-polymerase chain reaction (RT-PCR)

The COX-2 relative expression in vascular endothelial cells was in-depth measured through the real time RT-PCR according to the instructions of manufactures. Briefly, the New Zealand white rabbits were fed by using high-fat diet and treated with hypertension on one side of the renal artery stenosis at the aim of inducing the animal model of atherosclerosis. Then these two CPs were given for the indicated treatment with a concentration of 5 mg/kg. Subsequently, we isolated the atherosclerotic segment and then extracted overall RNA via the Trizol reagent. The RNA concentration was measured and then transcripted into cDNA for the detection of the levels of COX-2 in the vascular endothelial cells, *gapdh* was utilized as internal control gene. This experiment was performed three times or more, and obtained results were expressed as mean ± standard deviation.

2.7. Western blot

The western blot was implemented to detect the signaling pathway of Notch activation level in vascular endothelial cells after indicated treatment. This experiment was conducted according the protocols as previous described. New Zealand white rabbits were fed by using high-fat diet and treated with hypertension on one side of the renal artery stenosis to induce the animal model of atherosclerosis. Then these two CPs were given to perform the indicated treatment with a concentration of 5 mg/kg. Then, the vascular endothelial cells of the atherosclerotic segment were isolated for the total protein extraction. Protein samples were loaded onto the gel of sodium dodecyl sulfate (SDS) and then transferred onto the membranes of poly(1,1-difluoroethylene) (PVDF). After incubated with primary and secondary antibody, the expression of the Notch was observed.

3. Results and discussion

3.1. Molecular structure

CP **1** was hydrothermally synthesized via $Cu(NO_3)_2{\cdot}6H_2O$ reacting with NaOH, trz and H_3L, which was completely characterized via single crystal X-ray powder diffraction (PXRD), fourier transform infrared spectrometer (FT-IR) and the analysis of element. In accordance with the data of crystal which harvested under the ambient temperature, the refinement along with structural solution results indicated that the CP **1** is crystallized in monoclinic $P2_1/c$ space group and CP **1**'s minimum asymmetric unit is composed of 2.5 crystallographic independent Cu(II) centers in crystal, a L^{3-}, two ligands aqua, two trz^- and two molecules of lattice-water. As revealed in the Fig. 1a, Cu1 atom possesses a distorted geometry of octahedron with a chromophore of CuN_4O_2 and it is coordinated via two carboxylic acid O atoms in two H_3L (O7A and O7) in axial positions and four N atoms in four trz (N1A, N1, N4A and N4) in equatorial plane. Cu2 atom reveals a geometry of trigonal biyramid with one chromophore of CuN_2O_3 and it is coordinated via two carboxylic acid O atoms in two H_3L (O6 and O3), an O atom in one coordinated water (O2W) and two N atoms in two trz (N5 and N2). Cu3 atom also reveals a geometry of trigonal biyramid with one chromophore of CuN_2O_3 and it is coordinated via two N atoms in two carboxylic acid O atoms in two H_3L (O2 and O1), an O atom in one coordinated water (O1W) and two trz (N6 and N3). Cu1, Cu2 as well as symmetry-related Cu2A are combined via four molecules of trz (N1AN2A, N1N2, N4AN5A and N4N5) and two carboxylic groups of two ligands of H_3L (O6AO7A and O6O7) to form the linear trinuclear moiety of $[Cu_3N_8O_4]$. Each of the ligand L^{3-} with the coordination pattern μ_4-η^1:η^1:η^1:η^0:η^1:η^1 links two trinuclear clusters $[Cu_3N_8O_4]$ and a Cu3 atom in three directions in order to generate the infinite two-dimensional layer framework

Table 3
The reaction of distinct benzaldehyde derivatives with malononitrile catalyzed via CP **2**.

Entry	Substrate	Product	Conversion (%)
1	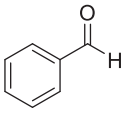	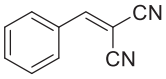	>99
2	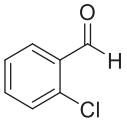	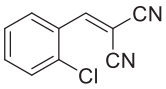	>99
3	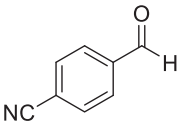	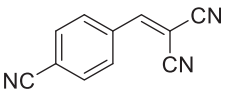	>99
4	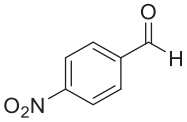	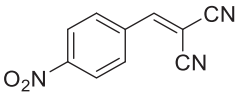	>99
5	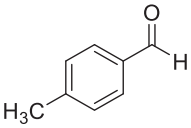	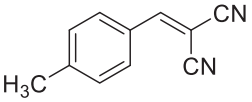	96
6	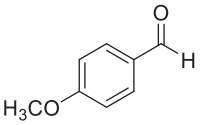	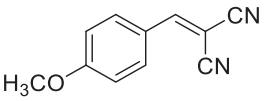	60
7	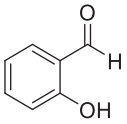	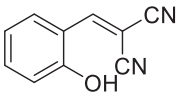	88
8	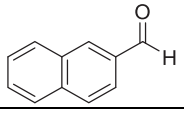	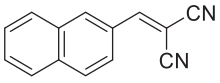	>99

(Fig. 1b). Then the two-dimensional layers are in-depth pillared with ligands trz to obtain the final three-dimensional skeleton (Fig. 1c). In terms of topology, each of the trinuclear clusters [$Cu_3N_8O_4$] is connected with four ligands of L^{3-} and four ligands of trz^-, which could be regarded as an eight-linked node; each of Cu3 atom links a ligand L^{3-} and two ligands of trz^- and could be viewed as three-linked node; each of ligand L^{3-} links two clusters [$Cu_3N_8O_4$] and a Cu3 atom, which can be regarded as a three-linked node; whereas each of the ligand trz^- can be viewed as a linear connector between the Cu3 atom and [$Cu_3N_8O_4$] clusters. Based on this simplification, CP **1** has a three-dimensional (3,8)-linked net. The topology analysis via the program of TOPOS indicates the (3,8)-linked net with topology of $(5^3)_2(5^8{\cdot}6^4{\cdot}7^8{\cdot}8^4{\cdot}9^4)$ (Fig. 1d).

The analysis of X-ray structure exhibits that CP **2** is crystallized in monoclinic $P2_1/c$ space group and there are an absolute Cu(II) atom in crystal, a ligand of HL^{2-} and a biz co-ligand in CP **2**'s asymmetric unit (Fig. 2a). As exhibited in the Fig. 2a, Cu(II) atom is located in the coordination geometry of tetrahedron with three carboxylic acid O atoms (O3B, O2A and O1) of three ligands H_3L and a N atom (N1) of a ligand biz. Each of the biz ligand reveals as a terminal ligand, which binds to a Cu(II) atom in the monodentate pattern, whereas each of ligand HL^{2-} links three Cu(II) atoms via two carboxylic group. And coordination pattern for the ligand of HL^{2-} can be expressed as the μ_3-η^1:η^1:η^1:η^0:η^0:η^0 (Fig. 2b). It should be noted that the carboxybenzyloxy group of the ligand is free coordination without deproton. Two corresponding Cu(II) atoms in crystal are bridged via a pair of carboxylic acid group of ligand HL^{2-} to form a cluster [$Cu_2(CO_2)_2$], where the distance of Cu···Cu is 4.209(2) Å. Then a N atom of ligand biz and a carboxylic acid O atom of ligand HL^{2-} are combined with each Cu(II) atom of cluster [$Cu_2(CO_2)_2$] to obtain SBUs [$Cu_2(CO_2)_2O_2N_2$] based on Cu_2. In addition, the ligand HL^{2-} links SBUs based on Cu_2 to generate a two-dimensional layer framework (Fig. 2b and c). The unprotonated carboxybenzyloxy groups alternately point up and down to two-dimensional tablet. The dicarboxyphenyl groups in the ligand of HL^{2-} are twisted via the carboxybenzyloxyl groups, and its dihedral angles is 9.1(2)°. In the terms of topology, each of the ligand HL^{2-} can be viewed as a linear connector between SBUs based on Cu_2; whereas each of SBUs based on Cu_2 is connected with four ligands HL^{2-} and can be regarded as a four-linked node, the entire structure for CP **2** is the extended neutral four-linked network (Fig. 2d).

In comparison with the incomparable characteristics of CPs and the demand of the novel generation of increased heterogeneous catalysts, the development of the environmentally friendly Knoevenagel condensation CP catalyst has become a research hotspot in past few years. The condensation reactions of Knoevenagel are the familiar organic reaction, which is mainly used to generate C—C bonds and to synthesize significant derivatives for different purposes. In accordance with the former reports, condensation reaction of Knoevenagel is commonly catalyzed via Lewis acid-base positions or Lewis base. In consideration with the architecture of CP **2** involves uncoordinated nitrogen atoms in ligand benzimidazole (Lewis base positions) and protonated carboxylic groups (Lewis acid positions) while these active sites are absent in the CP **1**, we try to use CP **2** to catalyze this reaction. The optimum conditions of reaction were explored with malononitrile and benzaldehyde as the

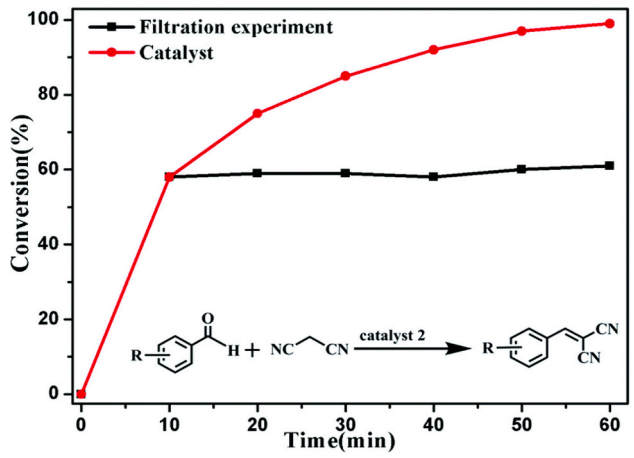

Fig. 3. The experiments of hot filtration (black) and Kinetic (red) catalyzed via CP **2**. (For interpretation of the references to colour in this figure legend, the reader is referred to the web version of this article.)

substrates (Table 2). First of all, blank experiment was carried out in the inexistence of catalyst for 60 min at 60 °C (entry 1), and only 18% of the product was produced. And then, in order to determine catalytic site, H_3L of 3 mg or ligand benzimidazole of 2 mg were utilized as the homogeneous catalysts, and medium conversions (52% and 46%, entry 2 and entry3) were achieved. Afterward, with catalyst amount was enhanced from 3 mg to 5, 8 and 10 mg, the conversions respectively enhanced from 39% to 82% and 94% as well as >99% (entries 4, 5, 6 and 7). Therefore, following reactions are carried out at distinct temperatures with the identical amount of catalyst, 10 mg. At RT, only 33% of the conversion was realized (entry 8). Via increasing the temperature to 40 °C, 50 °C and 60 °C, and the conversion respectively increase to 83%, 96% and >99% (entries 9, 10 and 7). At the aim of studying the effect of solvents on the reaction, experiments were implemented in diverse solvents for instance, acetone, ethanol, toluene and dichloromethane. The results show that conversion were much lower than that without solvent (entries 11, 12, 13, 14). To make a comparison, the catalytic performances of the Htrz and CP **1** toward the Knoevenagel condensation reaction were also studied under a similar reaction condition of CP **2**. As indicated in entries 15 and 16, the Htrz shows a moderate conversion due to its three N-donor sites. However, the conversion for CP **1** is only 20%, which is similar to the value of the blank experiments, indicating it shows little catalytic activity toward the Knoevenagel condensation reaction due to the lack of uncoordinated N sites as well as its tightly packed 3D framework structure.

In order to study the catalytic universality for CP **2**, the reactions were performed for 60 min at 60 °C without solvent. The reaction of a series of malondialdehyde without functionalized benzaldehyde derivatives was studied (Table 3). The results show that the conversion of benzaldehyde with substituted electron absorption parts (such as 4-NO_2, 4-CN and 2-Cl) can up to 99% (entries 2, 3, 4). However, when substituent was replaced via the electron-donating group (*such as* 4-CH_3, 4-CH_3-O or 2-OH), conversions is respectively reduced by 96%, 60% and 80% (entries 5, 6, 7). This phenomenon is due to substituents electronic effect. When the steric hindrance 2-naphthalene formaldehyde is used as the substrate, the conversion rate is as high as 99% (entry 8). The results reveal that catalytic activity for CP **2** is chiefly affected via the electronic influence.

The reaction rate was investigated via the kinetic experiment of CP **2**. We monitor the conversion rate by gas chromatography every 10 min (Fig. 3). In first 10 min, the reaction rate was the highest. Second, the rate kept growing rapidly, reaching 92% 40 min later. Afterward, gradual growth was found in next 20 min, reaching 99% in 60 min. In order to study whether it was the reaction of heterogeneous catalysis, the crystals for CP **2** were filtered 10 min later. And then, filtrate was stirred for another 40 min under the identical conditions. The Benzylidene methacrylonitrile yield did not increase, indicating that the reaction of catalysis was heterogeneous.

3.2. CP increased the values of the PT and APTT

There was usually combined with a dysregulated coagulation in the atherosclerotic segment during the procession of atherosclerosis. Thus, in this experiment, after the synthesis of CPs **1** and **2**, activated partial thromboplastin time (APTT) and prothrombin time (PT) was evaluated in this experiment. According to the resultsof Fig. 4, we can find that there was a reduced PT and APTT value in the model groups, indicating the coagulation was over activated in the atherosclerosis disease. While, after CP **1** treatment, the PT and APTT values were increased significantly, suggesting the over activated coagulation in the atherosclerotic segment was reversed. But CP **2** showed no promotion on the dysregulated coagulation.

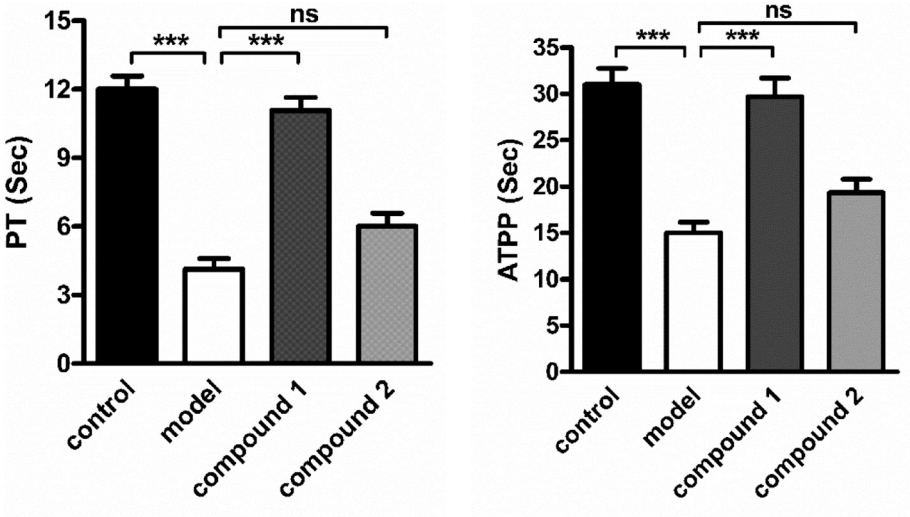

Fig. 4. Increased values of the PT and APTT after treated by the CP. The animal model of atherosclerotic was established on New Zealand white rabbits, and one of these two CPs was given to implement the indicated treatment with a concentration of 5 mg/kg. The values of the PT and APTT after CP treatment were determined. Control refers to the normal animal, the model refers to the atherosclerotic animal model.

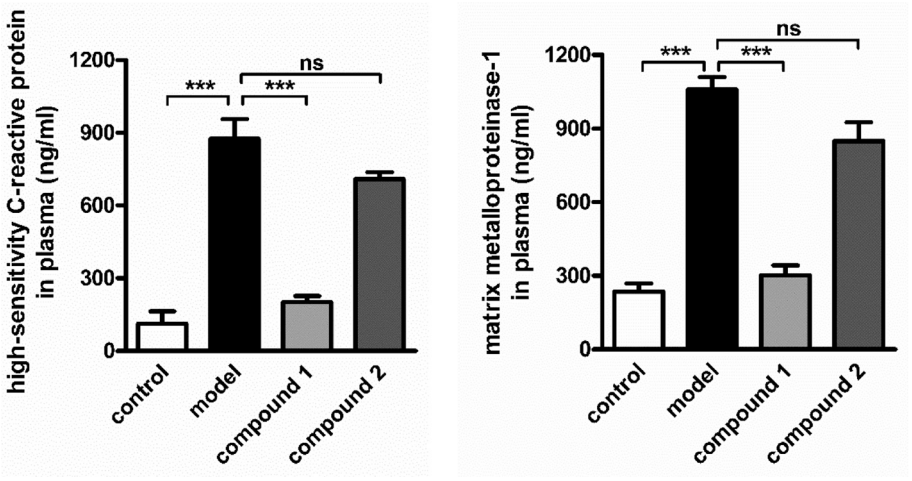

Fig. 5. Reduced content of inflammatory mediator released by the atherosclerotic segment. Atherosclerotic animal model was constructed on New Zealand white rabbits, and one of these two CPs was given to implement the indicated treatment with a concentration of 5 mg/kg. The content of inflammatory mediator released by the atherosclerotic segment detected via the ELISA test kit. Control refers to the normal animal, the model refers to the atherosclerotic animal model.

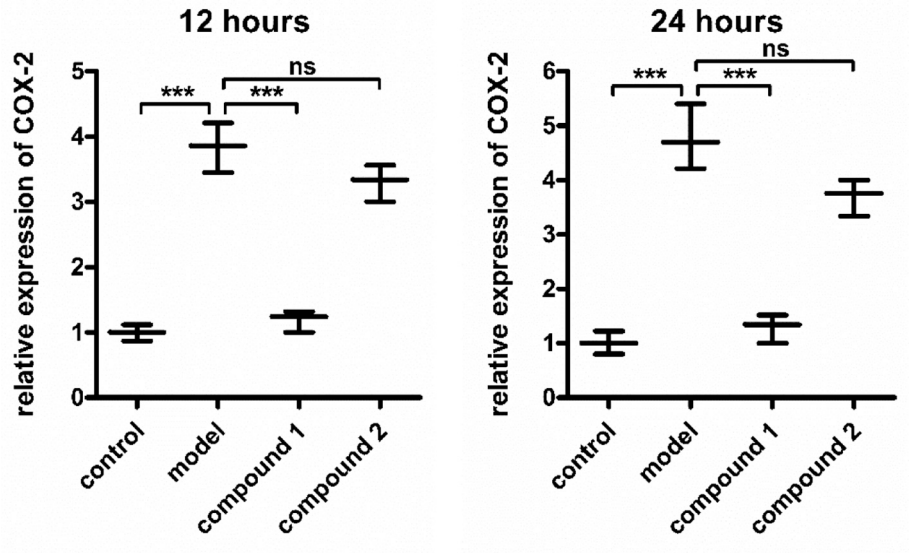

Fig. 6. Suppressed the COX-2 relative expression in the vascular endothelial cells after treated by the CP. The animal model of the atherosclerotic was built on New Zealand white rabbits, and one of these two CP was given to implement the indicated treatment with a concentration of 5 mg/kg. RT-PCR was implemented to detect the COX-2 relative expression in the vascular endothelial cells. Control refers to the normal animal, the model refers to the atherosclerotic animal model.

3.3. CP reduced the content of inflammatory mediator released by the atherosclerotic segment

In the recent years, the high-sensitivity C-reactive protein and matrix metalloproteinase-1 released by the atherosclerotic segment were widely used as the indicator for the atherosclerosis evaluation. So, in this study, the effect of these two CPs against the atherosclerosis was detected via the ELISA assay. The results revealed in the Fig. 5 indicated that there was an obvious enhance level of the high-sensitivity C-reactive protein and matrix metalloproteinase-1 in the plasma, which could be obviously reversed by CP **1** treatment. However, CP **2** exhibited no influence of the inflammatory mediator releasing.

3.4. CP suppressed the relative expression of the COX-2 in vascular endothelial cells

In the previous research we have demonstrated the outstanding inhibition of the CP **1** against the inflammatory mediator releasing. And the COX-2 in vascular endothelial cells could also regulated the inflammatory mediator synthesis and production, so the COX-2 relative expression in the vascular endothelial cells will be measured with real time RT-PCR. From Fig. 6, we obtained this information, in model group, the CP **1** possesses stronger suppression ability on reversing the COX-2 abnormal expression.

3.5. CP suppressed the Notch signaling pathway activation in the vascular endothelial cells

As previous reported, the signaling pathway of Notch possesses a significant function in the anti-inflammatory responses in the cells. After CP **1** or CP **2** treatment, the signaling pathway of Notch activation level in vascular endothelial cells was assessed by the western blot. We can see that in consistence with previous results, in model group, the Notch signaling pathway activation was much higher in comparison with control group. Under CP **1** treatment, the Notch signaling pathway activation was reduced, and CP **2** possesses no influence against

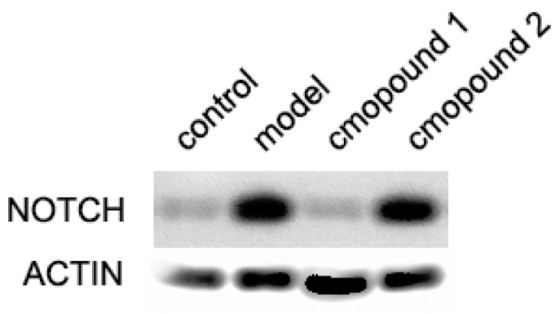

Fig. 7. Suppressed Notch signaling pathway activation in the vascular endothelial cells under CP exposure. Atherosclerotic animal model was constructed on New Zealand white rabbits, and one of these two CP was given to implement the indicated treatment with a concentration of 5 mg/kg. Notch signaling pathway activation in vascular endothelial cells was determine by the western blot.

pathway activation (Fig. 7).

4. Conclusion

In summary, by altering auxiliary nitrogen-donor ligands, two coordination polymers have been triumphantly produced under the conditions of hydrothermal. The study of single crystal diffraction of X-ray reflects that the CP **1** possesses a three-dimensional (3,8)-linked net with topology $(5^3)_2(5^8{\cdot}6^4{\cdot}7^8{\cdot}8^4{\cdot}9^4)$, whereas CP **2** reveals a two-dimensional layer four-linked net. The CP **2** with both acidic and basic sites was investigated as heterogeneous catalyst, which reveals the highly efficient catalytic propert of the condensation reaction of Knoevenagel. CP **1** has a stronger improvement on the coagulation parameters during atherosclerosis in comparison with the CP **2**. Furthermore, ELISA assay also exhibited that the CP **1** could obviously decrease the inflammatory mediator released by the atherosclerotic segment, but not CP **2**. Following that, the COX-2 in vascular endothelial cells was also inhibited by CP **1** instead of CP **2**. Eventually, western blot indicated that the CP **1** possess stronger effect against inhibiting the Notch signaling pathway. In conclusion, different from the CP **2**, CP **1** possesses stronger treatment effect against atherosclerosis by regulating the COX-2 in the vascular endothelial cells and reducing the inflammatory responses.

Author statement

Yong-Chang Zhao and Yan Zhang conceived and designed the experiments;

De-Ying Jiang and Liang Wang performed the experiments;

Ping Sun wrote the paper.

Declaration of Competing Interest

The author(s) declare(s) that there is no conflict of interest regarding the publication of this paper.

Acknowledgments

Not applicable.

Appendix A. Supplementary data

Supplementary data to this article can be found online at https://doi.org/10.1016/j.jinorgbio.2021.111464.

References

[1] H. Wang, Z.Y. Nie, M. Liu, R.R. Li, L.H. Huang, Z. Lu, L.J. Jin, Y.X. Li, Clinical characteristics of perivascular space and brain CT perfusion in stroke-free patients with intracranial and extracranial atherosclerosis of different extents, Ann. Transl. Med. 8 (2020) 215.

[2] Q. Zheng, L. Pan, Y. Ji, H_2S protects against diabetes-accelerated atherosclerosis by preventing the activation of NLRP3 inflammasome, J. Biomed. Res. 34 (2019) 94–102.

[3] S. Xu, J. Weng, Familial hypercholesterolemia and atherosclerosis: animal models and therapeutic advances, Trends Endocrinol. Metab. 31 (2020) 331–333.

[4] K. Wang, X. Ma, D. Shao, Z. Geng, Z. Zhang, Z. Wang, Coordination-induced assembly of coordination polymer submicrospheres: promising antibacterial and in vitro anticancer activities, Cryst. Growth Des. 12 (2012) 3786–3791.

[5] S. Mukherjee, S. Ganguly, K. Manna, S. Mondal, S. Mahapatra, D. Das, Green approach to synthesize crystalline nanoscale Zn II -coordination polymers: cell growth inhibition and immunofluorescence study, Inorg. Chem. 57 (2018) 4050–4060.

[6] C. Guo, Y. Zhang, L. Zhang, Y. Zhang, J. Wang, 2-Methylimidazole-assisted synthesis of a two-dimensional MOF-5 catalyst with enhanced catalytic activity for the Knoevenagel condensation reaction, CrystEngComm 20 (2018) 5327–5331.

[7] Z. He, X. Zhao, X. Pan, Y. Li, X. Wang, H. Xu, Z. Xu, Ligand geometry controlling Zn-MOF partial structures for their catalytic performance in Knoevenagel condensation, RSC Adv. 9 (2019) 25170–25176.

[8] K. Cai, W. Tan, N. Zhao, H. He, Design and assembly of a hierarchically micro- and mesoporous MOF as a highly efficient heterogeneous catalyst for Knoevenagel condensation reaction, Cryst. Growth Des. 20 (2020) 4845–4851.

[9] C.I. Ezugwu, B. Mousavi, M.A. Asraf, Z. Luo, F. Verpoort, Post-synthetic modified MOF for Sonogashira cross-coupling and Knoevenagel condensation reactions, J. Catal. 344 (2016) 445–454.

[10] D. Rambabu, M. Ashraf, A. Gupta Pooja, A. Dhir, Mn-MOF@Pi composite: synthesis, characterisation and an efficient catalyst for the Knoevenagel condensation reaction, Tetrahedron Lett. 58 (2017) 4691–4694.

[11] Y. Luan, Y. Qi, H. Gao, R.S. Andriamitantsoa, N. Zheng, G. Wang, A general post-synthetic modification approach of amino-tagged metal–organic frameworks to access efficient catalysts for the Knoevenagel condensation reaction, J. Mater. Chem. A 3 (2015) 17320–17331.

[12] A. Das, N. Anbu, S.K. Mostakim, A. Dhakshinamoorthy, S. Biswas, A functionalized UiO-66 MOF for turn-on fluorescence sensing of superoxide in water and efficient catalysis for Knoevenagel condensation, Dalton Trans. 48 (2019) 17371–17380.

[13] M.E. Bravo-Gómez, J.C. García-Ramos, I. Gracia-Mora, L. Ruiz-Azuara, Antiproliferative activity and QSAR study of copper(II) mixed chelate [Cu(N–N)(acetylacetonato)]NO_3 and [Cu(N–N)(glycinato)]NO_3 complexes, (Casiopeínas®), J. Inorg. Biochem. 103 (2009) 299–309.

[14] L. Ruiz-Azuara, M.E. Bravo-Gomez, Copper compounds in cancer chemotherapy, Curr. Med. Chem. 17 (2010) 3606–3615.

[15] T. Sabithakala, V.R.R. Chittireddy, DNA binding and in vitro anticancer activity of 2-((1 H -benzimidazol-2-yl)methylamino)acetic acid and its copper(II) mixed-polypyridyl complexes: synthesis and crystal structure, Appl. Organomet. Chem. 32 (2018), e4550.

[16] Z. Tohidiyan, I. Sheikhshoaie, M. Khaleghi, J.T. Mague, A novel copper (II) complex containing a tetradentate Schiff base: synthesis, spectroscopy, crystal structure, DFT study, biological activity and preparation of its nano-sized metal oxide, J. Mol. Struct. 1134 (2017) 706–714.

[17] N. Shahabadi, A.R. Abbasi, A. Moshtkob, F. Shiri, DNA-binding studies of a new Cu (II) complex containing reverse transcriptase inhibitor and anti-HIV drug zalcitabine, J. Coord. Chem. 72 (2019) 1957–1972.

[18] G. Crisponi, V.M. Nurchi, J.I. Lachowicz, M. Crespo-Alonso, M.A. Zoroddu, M. Peana, Kill or cure: misuse of chelation therapy for human diseases, Coord. Chem. Rev. 284 (2015) 278–285.